



# EXPERIMENTAL INVESTIGATION ON HEAT TRANSFER CHARACTERISTICS OF SUPERCRITICAL CARBON DIOXIDE FLOWING IN HORIZONTAL AND VERTICAL MICROTUBES

Efe Öztabak<sup>1</sup>, Oğuzhan Gökkaya<sup>1</sup>, Hojin Ahn<sup>1\*</sup>

<sup>1</sup>Department of Mechanical Engineering, Yeditepe University, Istanbul, 34755, Turkey

## ABSTRACT

The heat transfer characteristics of supercritical carbon dioxide (sCO<sub>2</sub>) at 8.0 MPa through a microtube, 0.509 mm in diameter, have experimentally been investigated under the constant heat flux boundary condition. The effect of three different flow configurations (namely, horizontal, upward, and downward flows) on heat transfer activity has been studied for both laminar and turbulent flows. For laminar flow, the behavior of the Nusselt number is found to be highly dependent on the flow configuration and thus on the direction of the buoyancy force. For horizontal flows, only a single peak of the Nusselt number is observed. For downward flow, however, three peaks of the Nusselt number appear as the mass flux increases, while the Nusselt number for upward flow is characterized by two peaks at low mass flux. The physical mechanism of the multiple peaks in laminar flow is believed to be the fluid mixing between the wall boundary and core region. On the other hand, turbulent flow is characterized by only a single peak of the Nusselt number for all flow directions. The magnitude of the modified Richardson number of turbulent flows is found to be much smaller than that of laminar flows. Therefore, it is concluded that the buoyancy force significantly affects the heat transfer characteristics of laminar flows while little affecting those of turbulent flows.

## 1. INTRODUCTION

The heat transfer characteristics of supercritical carbon dioxide (sCO<sub>2</sub>) have lately been investigated due to its potential applications in micro-scale heat exchangers for cooling microdevices, nuclear cooling systems, and the Brayton power cycle. It is a great challenge to fully understand the cooling and heating of sCO<sub>2</sub> since the thermophysical properties rapidly change near the critical point. Moreover, microtubes are capable of dissipating heat up to fifty-fold of conventional tubes [1]. Thus, the use of sCO<sub>2</sub> as a low-cost and environment-friendly working fluid to cool micro-devices requires the investigation of its heat transfer characteristics in microtubes. However, there is no experimental study on laminar flow ( $Re < 1,000$  at the inlet) through a microtube, less than 1 mm in diameter, in the literature. We believe that this is caused by the difficulties of experimental work in the microscale with reasonable uncertainties.

There are some numerical studies available in the literature on laminar flows through microtubes. Cao et al. [2] numerically investigated flows through a horizontal microtube, 0.5 mm in diameter, under a cooling condition where the Reynolds number at the inlet is 1866. Another numerical study has been conducted by Yang et al. [3] to investigate the flow through a tube that has an inner diameter of 0.5 mm at different inclination angles. Liao and Zhao [4] have also employed a numerical method to examine sCO<sub>2</sub> flows through vertical microtubes at  $Re = 658$  and 2060 in different sizes.

In this study, heat transfer characteristics of sCO<sub>2</sub> through a microtube, 0.509 mm in diameter and 301 mm in heating length, are examined for horizontal, upward, and downward flows at 8.0 MPa under the constant heat flux boundary condition in both laminar and turbulent flow regimes.

\*Corresponding Author: [erdeman@yeditepe.edu.tr](mailto:erdeman@yeditepe.edu.tr)

## 2. EXPERIMENTAL SYSTEM

Figure 1 shows the schematic of the experimental setup that consists of a CO<sub>2</sub> tank, a syringe pump, a vacuum pump, a Coriolis type flowmeter, two DAQ (data acquisition) systems, two absolute pressure sensors, and the test section. The secondary CO<sub>2</sub> tank is used to provide constant pressure downstream of the test section. A precise needle valve is placed at the outlet of the test section to control the mass flow rate in the system. The microtube is located in a vacuum chamber where the absolute pressure is kept at less than 1 kPa during the experiments by a vacuum pump to reduce the convective heat loss on the outer surface of the tube. In addition, the microtube is enveloped by a radiation shield to minimize radiational heat loss. A PT100 sensor measures the fluid mean temperature in the mixing chamber at the tube inlet. Total 29 T-type thermocouples are attached to the microtube and two more thermocouples have been used to measure the ambient temperature. The microtube is heated by a direct current. Local heat generation along the tube is calculated from the electric current and the electrical resistivity of the tube wall. Thus, the present study calculates the net heat flux to the fluid by considering the local heat generation, heat loss from the outer surface, and axial conduction along the tube. Then, the fluid mean enthalpy through the microtube is obtained by integrating the net heat flux over each interval between two adjacent thermocouples as shown in Eq. (1). Accordingly, the mean temperature through the microtube is obtained from the known mean enthalpy by using NIST REFPROP software [5]. Finally, the results are described in terms of mass flux,  $G$ , which is the ratio of mass flow rate to the flow area since the Reynolds number significantly increases from the tube inlet to the outlet.

$$h_{k+1} = h_k + \frac{\pi d_i}{\dot{m}} \int_k^{k+1} q''_{net} dx \quad (1)$$

The uncertainty propagation of each measured variable is calculated, and the total uncertainty in the Nusselt number is determined to be 4 to 10% for all cases, following the procedure by [6].

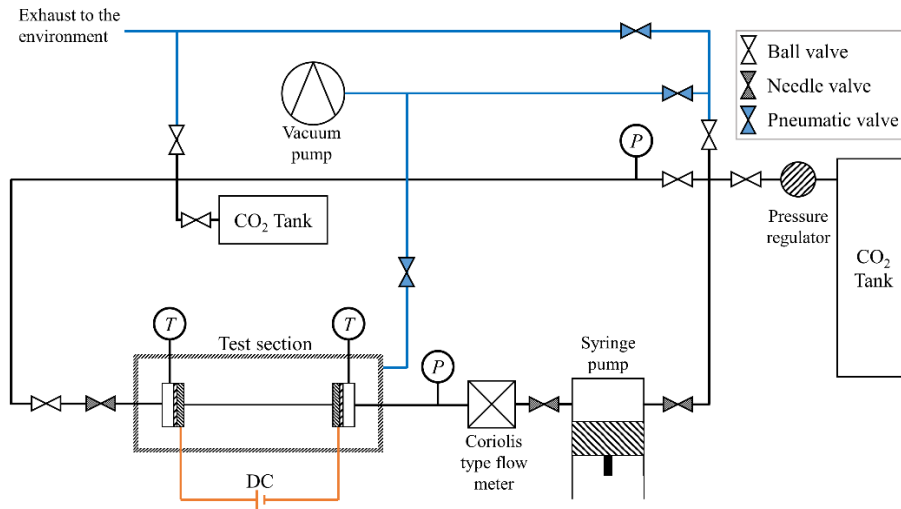


**Figure 1:** Schematic of the experimental setup

## 3. RESULTS AND DISCUSSION

Figure 2 compares three different flow configurations, namely, horizontal, upward, and downward, for the mass fluxes of 60 and 140 kg/m<sup>2</sup>s. Only a single peak is observed for the horizontal flow cases whereas there are multiple peaks for upward and downward flows depending on the configuration. Though all data with different  $q''/G$  and  $G$  values are not presented here, their general characteristics are described as follows. For upward flows, the Nusselt number has a single local peak for low  $q''/G$ , and the second peak arises as  $q''/G$  increases as shown in Figure 2 (a). The first peak approaches the

tube inlet as  $G$  grows for a given  $q''/G$ , whereas the second peak diminishes as it is pushed out to the tube outlet (see Figure 2 (b)). For downward flows, however, the Nusselt number has a single local peak for low mass fluxes regardless of  $q''/G$  values. On the other hand, three local peaks of the Nusselt number are found at high  $G$  as shown in Figure 2 (b).

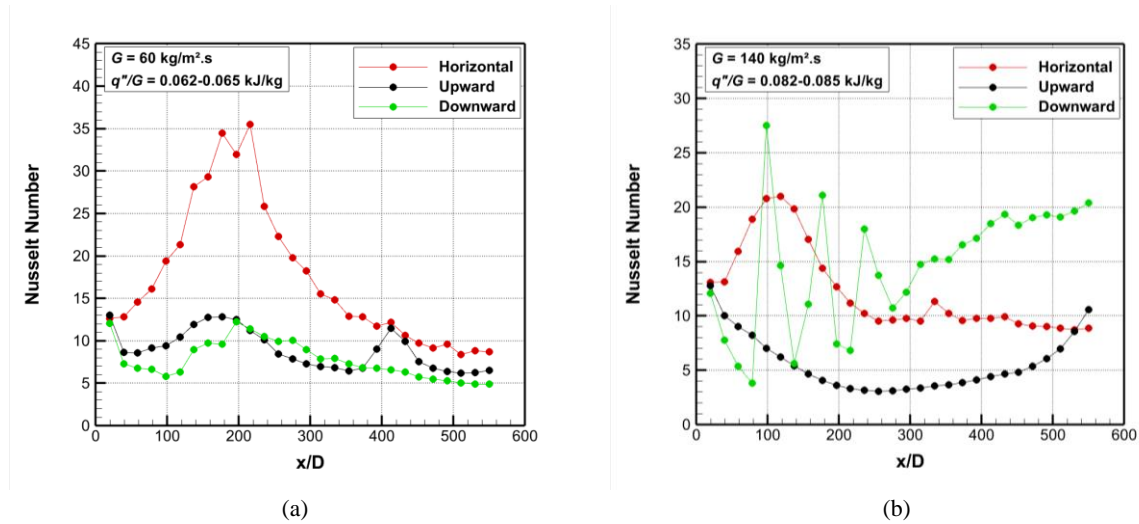


**Figure 2:** The variation of the Nusselt number at the mean temperature through the microtube as a function of  $x/d$  for the case of (a)  $G = 60 \text{ kg/m}^2\text{s}$  and  $q''/G = 0.062\text{-}0.065 \text{ kJ/kg}$  (b)  $G = 140 \text{ kg/m}^2\text{s}$  and  $q''/G = 0.082\text{-}0.085 \text{ kJ/kg}$  at 8.00 MPa

The cases of turbulent flows are examined in Figure 3. Different from the laminar cases, the heat transfer characteristics of turbulent flow are shown to be similar for all cases of upward, downward, and horizontal flows for given mass and heat fluxes. The magnitudes of the Nusselt number are found to be independent of flow configurations as shown in Figure 3 (a). As expected, the Nusselt number increases with the increasing mass flux. Furthermore, while the multiple peaks of the Nusselt number are possible in laminar flow, the turbulent flow is characterized by only a single peak of the Nusselt number regardless of flow configuration. Figure 3 (b) shows that, as the heat flux increases with the mass flux kept constant, the peak location moves toward the inlet, and the magnitude of the peak decreases.

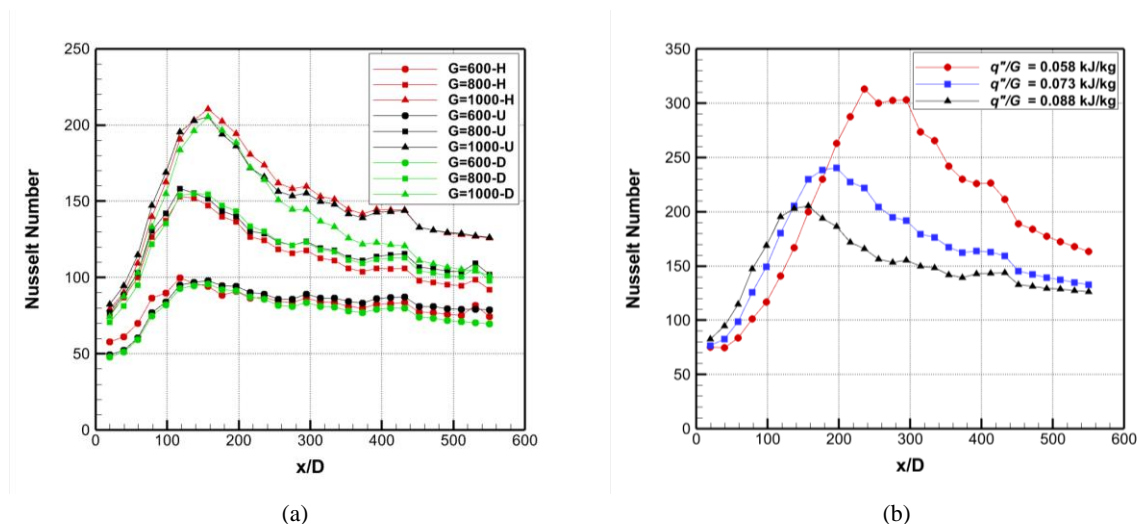


**Figure 3:** The variation of the Nusselt number at the mean temperature through the microtube as a function of  $x/d$  for the case of (a)  $G = 600, 800, \text{ and } 1000 \text{ kg/m}^2\text{s}$  for horizontal, upward, and downward flows where  $q''/G = 0.085\text{-}0.088 \text{ kJ/kg}$  at 8.0 MPa (“H”, “U”, and “D” denote horizontal, upward and downward, respectively.), (b)  $G = 1000 \text{ kg/m}^2\text{s}$  for upward flow with  $q''/G = 0.058, 0.073 \text{ and } 0.088 \text{ kJ/kg}$

The modified Richardson number for the constant heat flux boundary condition, as shown in Eq. (2), is employed to examine the physical mechanism underlying the multippeak phenomenon. The modified Richardson number is considered a measure of buoyancy effect on mixed convection.

$$Ri^* = \frac{Gr^*}{Re^2} = \frac{Gr \cdot Nu}{Re^2} \quad (2)$$

The effect of buoyancy on the heat transfer characteristics of downward flow is examined in Figure 4 for the case of  $G = 140 \text{ kg/m}^2\text{s}$  with  $Re = 1020$  at the tube inlet. Figure 4 (a) shows that the mean temperature monotonously increases as expected but the wall temperature rapidly varies up and down, resulting in the sharp peaks of the heat transfer coefficient. When temperature variations in Figure 4 (a) are carefully examined, the film temperature is reduced at the peaks of the heat transfer coefficient. This is possible only when the colder fluid at the core is mixed with the warmer fluid near the wall boundary. The Nusselt numbers evaluated at both the mean and film temperatures are plotted in Figure 4 (b). Though their magnitudes are slightly different due to the difference in thermal conductivity at the mean and film temperatures, their peaks occur at the same locations. The modified Richardson numbers evaluated at the mean and film temperatures are also plotted in Figure 4 (b). No obvious relationship is observed between the modified Richardson number at the mean temperature,  $Ri_m^*$ , and the Nusselt numbers. On the other hand, the peak locations of  $Nu$  well correlate with the local maximum locations of the modified Richardson number at the film temperature,  $Ri_f^*$ . This implies that the fluid mixing suggested by the decrease of the film temperature in Figure 4 (a) is prompted by large buoyancy forces indicated by the maximum  $Ri_f^*$  at the near wall. However, it is noted that the first local maximum of  $Ri_f^*$  does not enhance the heat transfer. For upward flows, although not presented here, the first peak of  $Nu$  in Figure 2 (a) occurs around where  $Ri_f^*$  has a maximum. Therefore, the first peak must be related to the buoyancy effect near the wall as the film temperature approaches the pseudo-critical temperature. The second peak of  $Nu$  in Figure 2 (a) appears just after  $Ri_m^*$  reaches its maximum, indicating that the second peak occurs when fluid in the core approaches the pseudo-critical temperature.

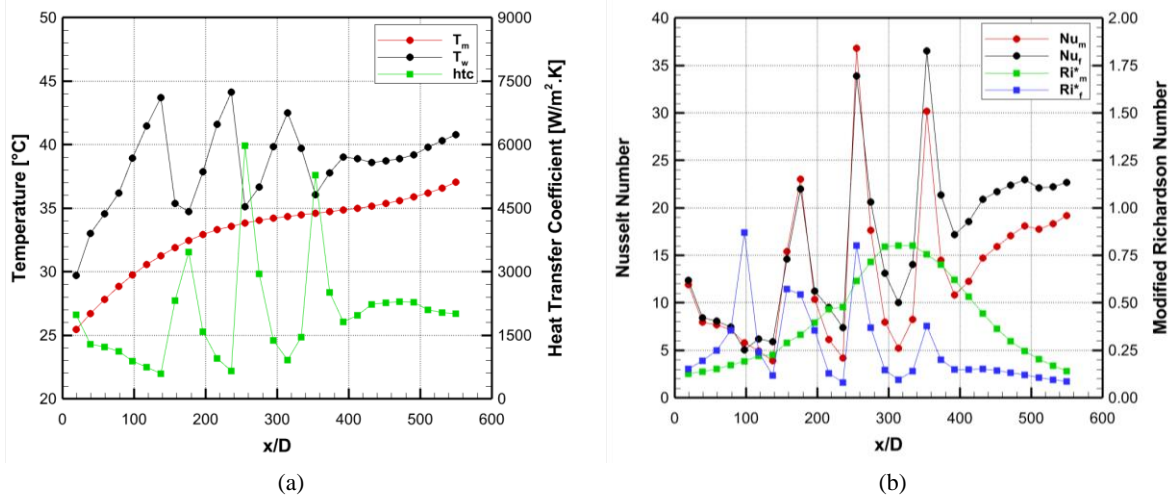


**Figure 4:** The variation of (a) the mean temperature, wall temperature, and heat transfer coefficient, (b) Nusselt number and modified Richardson number evaluated at both mean and film temperature, as a function of  $x/d$  for the case of  $G = 140 \text{ kg/m}^2\text{s}$  for downward flow where  $q''/G = 0.056 \text{ kJ/kg}$  at 8.0 MPa

The effect of buoyancy on the heat transfer activity for turbulent flow at  $G = 1000 \text{ kg/m}^2\text{s}$  is examined in Figure 5. Only a horizontal flow is considered since there is no significant difference between flow configurations. The heat transfer coefficient shown in Figure 5 (a) has a peak where the film temperature slightly exceeds the pseudo-critical temperature of 34.7°C at 8.0 MPa. Figure 5 (b) shows that the two Nusselt numbers evaluated at the mean and film temperature are quite different in

their magnitudes and peak locations because the thermal conductivity is a strong function of temperature. Note that, for laminar flow shown in Figure 4 (b), the peak locations of the Nusselt numbers at the mean and film temperatures are identical.

The relationship between the Nusselt number and the modified Richardson number is also examined in Figure 5 (b). While the laminar flow case of Figure 4 (b) has a single peak of  $Ri_m^*$  and multiple peaks of  $Ri_f^*$ , the turbulent case presented in Figure 5 (b) shows only a single peak of both  $Ri_m^*$  and  $Ri_f^*$ . Therefore, the single peak of the Nusselt number, whether it is evaluated at the mean temperature or at the film temperature, appears to be related to the single peak of the modified Richardson number.

It is noted that the peak magnitude of  $Ri^*$  for the laminar flow in Figure 4 is about five times greater than that of the turbulent flow in Figure 5. This shows that the buoyancy effect of the turbulent flow is weaker than that of the laminar flow. As a result, the heat transfer characteristics of turbulent flow are independent of the flow configurations as shown in Figure 3 (a). On the other hand, the buoyancy force affects laminar flow more dominantly, and thus the flow direction has a significant effect on the heat transfer characteristics as shown in Figure 2.

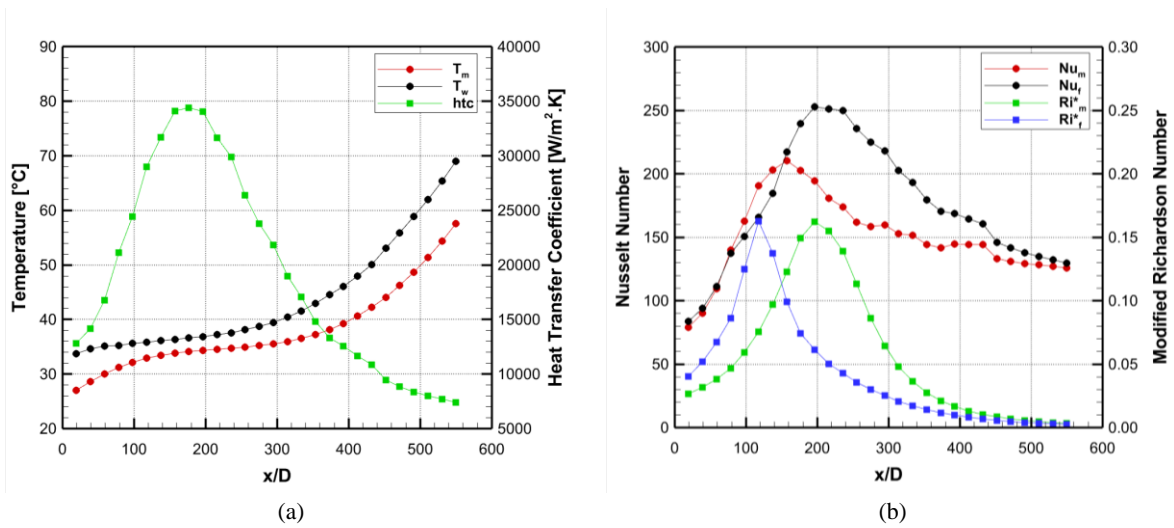


**Figure 5:** The variation of (a) the mean temperature, wall temperature, and heat transfer coefficient, (b) Nusselt number and modified Richardson number evaluated at both mean and film temperature, as a function of  $x/d$  for the case of  $G = 1000 \text{ kg/m}^2\text{s}$  for a horizontal flow where  $q''/G = 0.086 \text{ kJ/kg}$  at 8.0 MPa

#### 4. CONCLUSIONS

The present study has investigated heat transfer characteristics of both laminar and turbulent supercritical carbon dioxide flows through a microtube, 0.509 mm in diameter, at 8.0 MPa. For laminar flows in the horizontal configuration, a single peak of the Nusselt number is observed at the location where the film temperature slightly exceeds the pseudo-critical temperature (34.7°C). For downward flows, the Nusselt number has one local peak when the mass flux is low (60 kg/m<sup>2</sup>s) whereas the Nusselt number is characterized by three peaks for a higher mass flux (140 kg/m<sup>2</sup>s) due to the fluid mixing between the wall boundary and core region. For upward flow, on the other hand, the number of peaks in Nusselt number is two for low mass flux (60 kg/m<sup>2</sup>s) and the peaks disappear when the mass flux increases to 140 kg/m<sup>2</sup>s. The modified Richardson number which is a measure of buoyancy effect is employed to investigate multiple peaks. For downward flows, it is found that the modified Richardson number at the film temperature has a peak at the location where the Nusselt number reaches its local maximum. For upward flows, though not presented in this paper, the first peak of the Nusselt number appears when the modified Richardson number at the film temperature has a maximum. The second peak in the Nusselt number appears after the maximum of the modified Richardson number at the mean temperature. On the contrary, for turbulent flows, only one peak in the Nusselt number is observed

independent of the flow configuration. The peak is located where the film temperature is slightly above the pseudo-critical temperature. As the heat flux increases, the location of the peak in the Nusselt number moves toward the microtube inlet, and its magnitude decreases. When the mass flux is increased, it is shown that the magnitude of the Nusselt number at the peak location is augmented. The magnitude of the modified Richardson number in turbulent flows is found to be much smaller than that of laminar flows. In short, the heat transfer characteristics of laminar flow depend on the flow configuration and thus on the direction of the buoyancy force, and the modified Richardson number is relatively large. On the other hand, the heat transfer characteristics of turbulent flow are little affected by the flow configuration. Therefore, we conclude that the buoyancy force has a significant effect on laminar flows whereas it has little effect on turbulent flows.

## ACKNOWLEDGEMENTS

This work has been supported by The Scientific and Technological Research Council of Turkey (TÜBİTAK) [grant number 119M051]. We thank Mr. Ergin Bayrak for his interest in this research from the beginning. We are also grateful to Mr. Emirhan Şayhan for his help in building the CO<sub>2</sub> test setup.

## REFERENCES

- [1] T. Dixit & I. Ghosh, Review of micro- and mini-channel heat sinks and heat exchangers for single phase fluids. *Renew. Sustain. Energy Rev.*, **41** (2015) 1298–1311.
- [2] X.L. Cao, Z.H. Rao & S.M. Liao, Laminar convective heat transfer of supercritical CO<sub>2</sub> in horizontal miniature circular and triangular tubes. *Appl. Therm. Eng.*, **31** (2011) 2374–2384.
- [3] C. Yang, J. Xu, X. Wang & W. Zhang, Mixed convective flow and heat transfer of supercritical CO<sub>2</sub> in circular tubes at various inclination angles. *Int. J. Heat Mass Transf.*, **64** (2013) 212–223.
- [4] S.M. Liao & T.S. Zhao, A numerical investigation of laminar convection of supercritical carbon dioxide in vertical mini/micro tubes. *Prog. Comput. Fluid Dyn. An Int. J.*, **2** (2002) 144.
- [5] E.W. Lemmon, M.L. Huber & M.O. McLinden, NIST Standard Reference Database 23: Reference Fluid Thermodynamic and Transport Properties-REFPROP, Version 10.0. *National Institute of Standards and Technology, Standard Reference Data Program, Gaithersburg*, (2018).
- [6] R.S. Figliola & D.E. Beasley, *Theory and Design for Mechanical Measurements*. John Wiley & Sons, (2011), pp. 161–198, Hoboken, New Jersey.